Chemistry & Biodiversity

WILEY-VCH

CHEMISTRY & BIODIVERSITY

RESEARCH ARTICLE

ADME, Toxicity, Molecular Docking, Molecular Dynamics, Glucokinase activation, DPP-IV, α-amylase, and α-glucosidase Inhibition Assays of Mangiferin and Friedelin for Antidiabetic Potential

Ravikiran Maheshrao Suryawanshi[1] | Rupali Bhalchandra Shimpi[2] | V. Muralidharan[3] | Lalita Shashikant Nemade[4] | Simhachalam Gurugubelli[5] | Shahajan Baig[6] | Sunayana Rahul Vikhe[7] | Sachin A. Dhawale[8] | Mohammad Rakib Mortuza[9] | Sherouk Hussein Sweilam[10,11] | Falak A. Siddiqui[12] | Sharuk L. Khan[12] | Marco Tutone[13] | Irfan Ahmad[14] | Md. Zamshed Alam Begh[15]

[1]Department of Industrial Pharmacy and Quality Assurance, R. C. Patel Institute of Pharmaceutical Education and Research, Shirpur, Maharashtra, India | [2]Department of Pharmacognosy, R. C. Patel Institute of Pharmaceutical Education and Research, Shirpur, Maharashtra, India | [3]Department of Pharmaceutical Chemistry, Vishnu Institute of Pharmaceutical Education and Research, Hyderabad, India | [4]Department of Pharmaceutics, Govindrao Nikam College of Pharmacy, Sawarde, Maharashtra, India | [5]Internal Medicine Physician, Memorial Hospital, Gulfport, Mississippi, USA | [6]Department of Pharmacology, Government College of Pharmacy, Osmanpura, Chhatrapati Sambhaji Nagar, Maharashtra, India | [7]Department of Pharmacognosy, Pravara Rural College of Pharmacy, Loni, Maharashtra, India | [8]Department of Pharmaceutical Chemistry, Shreeyash Institute of Pharmaceutical Education and Research Aurangabad, Chhatrapati Sambhaji Nagar, Maharashtra, India | [9]Department of Chemistry and Biochemistry, Lamar University, Beaumont, Texas, USA | [10]Department of Pharmacognosy, College of Pharmacy, Prince Sattam Bin Abdulaziz University, Al-Kharj, Saudi Arabia | [11]Department of Pharmacognosy, Faculty of Pharmacy, Egyptian Russian University, Badr City, Cairo, Egypt | [12]Department of Pharmaceutical Chemistry, N.B.S. Institute of Pharmacy, Ausa, Maharashtra, India | [13]Dipartimento di Scienze e Tecnologie Biologiche Chimiche e Farmaceutiche, Università degli Studi di Palermo, Palermo, Italy | [14]Department of Clinical Laboratory Sciences, College of Applied Medical Science, King Khalid University, Abha, Saudi Arabia | [15]Department of Pharmacy, Faculty of Health and Life Sciences, Daffodil International University, Dhaka, Bangladesh

Correspondence: Falak A. Siddiqui (falakarjumand26@gmail.com) | Sharuk L. Khan (sharique.4u4@gmail.com)

Received: 25 October 2024 | **Revised:** 18 December 2024 | **Accepted:** 20 December 2024

Funding: The authors are thankful to the Deanship of Research and Graduate Studies, King Khalid University, Abha, Saudi Arabia, for financially supporting this work through the Large Research Group Project under Grant R.G.P.2/514/45.

Keywords: friedelin | glucokinase | in vitro enzymatic assay | mangiferin | α-amylase | α-glucosidase

ABSTRACT

Today the alarming situation of diabetes seeks innovative antidiabetic medications, especially those derived from natural sources, as natural substances are safer than manufactured pharmaceuticals. Therefore, this study investigated the inhibitory properties of mangiferin and friedelin against glucokinase (GK), dipeptidyl peptidase-IV (DPP-IV), α-amylase, and α-glucosidase using computational methods, in vitro enzyme assays, and in-depth ADMET analysis. The study utilized a computer-aided drug design approach to assess the potential therapeutic properties of mangiferin and friedelin as Type 2 diabetes mellitus (T2DM) therapeutic agents. Molecular docking studies' outcomes encouraged the evaluation of both compounds in in vitro enzymatic assays. The docking study results were validated with the help of molecular dynamics simulation. Mangiferin and friedelin showed that they activated GK 20% and 5% more than the basal activity of the enzyme, respectively. In the DPP-IV enzyme assay, mangiferin and friedelin demonstrated IC_{50} values (74.93 ± 0.71 and 110.64 ± 0.21 μg/mL, respectively) comparable with the reference compound sitagliptin. Moreover, mangiferin and friedelin showed IC_{50} comparable to acarbose against α-amylase (9.72 ± 0.15, 11.84 ± 0.06, and

10.19 ± 0.05 mg/mL, respectively). In the α-glucosidase enzyme assay, mangiferin, friedelin, and acarbose displayed 11.72 ± 0.10, 14.34 ± 0.02, and 9.14 ± 0.06 mg/mL of IC_{50} values, respectively. The compounds showed promising in silico ADMET and drug-likeness properties, with potential binding affinities with all enzymes. In vitro enzymatic assays showed mangiferin and friedelin activated GK 20% and 5% more than basal activity, with IC_{50} values comparable to acarbose.

1 | Introduction

Type 2 diabetes mellitus (T2DM) is a chronic medical disorder characterized by impaired insulin utilization or insufficient insulin production by the body. It is frequently associated with characteristics such as obesity and a sedentary lifestyle. In individuals with T2DM, elevated blood glucose levels can give rise to a range of health complications that can adversely impact the heart, kidneys, vision, and nerves if not well controlled. Adhering to a healthy diet and regular physical exercise are common lifestyle improvements often recommended as part of therapy. Moreover, if necessary, medicines or insulin may be prescribed to maintain optimal blood sugar levels and mitigate the risk of problems. Current oral care drugs for T2DM aim to decrease glucose synthesis in the liver, enhance glucose secretion, decrease glucose consumption, and promote glucose utilization [1–3]. The most commonly used drugs for T2DM are sulfonylureas, meglitinides, thiazolidinediones, biguanides, and α-glucosidase inhibitors. Most of these drugs, however, have undesirable side effects, including hypoglycemia and weight gain [4–6]. Several new classes of diabetes drugs have been developed in recent years. These include inhibitors of dipeptidyl peptidase-IV (DPP-IV), glucagon receptor antagonists, and sodium-glucose co-transporter 2; inhibitors of hepatic glucose metabolism; agonists of pancreatic G protein–coupled fatty acid receptors; and enhancers of insulin-releasing glucokinase (GK) [7, 8].

α-Amylase and α-glucosidase are essential enzymes in the metabolism of dietary carbohydrates in T2DM patients. They hydrolyze complex carbohydrates into glucose, which can lead to excessive blood sugar levels. Inhibiting these enzymes can effectively regulate blood glucose levels, potentially reducing post-meal blood glucose rise, making it a potential treatment strategy [9]. Treatment of T2DM using DPP-IV inhibitors has proven safe, effective, and well-acknowledged [1, 10–18]. According to the findings of a current study, GK activators, often known as GKAs, may provide a significant advantage to those suffering from T2DM [19–23]. The medical community urgently seeks innovative antidiabetic medications, especially those derived from natural sources, as natural substances are safer than manufactured pharmaceuticals. Two of these could be mangiferin and friedelin (Figure 1A). Mangiferin, also known as 1,3,6,7-tetrahydroxyxanthone-C_2-β-D-glucoside, a biologically active compound primarily obtained from the mango tree, is a biologically active compound. It exhibits strong antioxidant properties and has a range of pharmacological actions, such as reducing diabetes, inhibiting tumor growth, regulating fat metabolism, protecting the heart, reducing high uric acid levels, preserving nerve cells, and reducing inflammation and fever. As a result, it has several health-promoting qualities and offers a viable subject for future study and development [24–29]. The only compound with a friedelane skeleton known from the genus *Myrianthus*, particularly from the trunk wood of *Myrianthus serratus*, is friedelin (friedelan-3-one). In addition to having anti-inflammatory and gastro-protective properties, it is a precursor to crucial anticancer quinone methides [30–32]. The study investigated the inhibitory potential of mangiferin and friedelin against four enzymes in diabetes management. We used a computer-aided drug design approach, in vitro enzyme assays, and in-depth ADMET analysis. The significance of choosing these two compounds for the study is that these are from natural sources and have been reported for various phramacological activities. These compounds' specific target for antidiabetic activity can lead to the discovery of more novel compounds.

2 | Methods and Materials

2.1 | In Silico Drug-Like Profile

Drug-likeness qualities are crucial in drug discovery because they aid in identifying molecules with features favorable to effective therapeutic development. To find molecules with good pharmacokinetic profiles and low toxicity potential, scientists evaluate various characteristics, including molecular weight, lipophilicity, hydrogen bonding capability, and many more. Increasing the likelihood of discovering lead compounds with improved effectiveness, safety, and oral bioavailability and speeding up the development of new pharmaceuticals is possible by optimizing drug-likeness features early in the drug discovery process [33, 34]. The AMDETlab web server was upgraded to ADMETlab 2.0, which we used to predict the pharmacokinetics and toxic characteristics of selected natural compounds (https://admetmesh.scbdd.com/) [35].

2.2 | Molecular Docking

The molecular docking method used AutoDock Vina 1.1.2 software, PyRx Virtual Screening Tool 0.8 from Chimaera version 1.10.2, and BIOVIA Discovery Studio. The compounds' structures were retrieved from the US National Library of Medicine's PubChem database (https://pubchem.ncbi.nlm.nih.gov/). Energy reduction was carried out using the universal force field (UFF) [36]. We obtained the three-dimensional crystal structures of the enzymes from the RCSB Protein Data Bank (PDB) (https://www.rcsb.org/).

To validate the docking method, we have re-docked the native ligands present in each crystal structure. The results of these interactions were then compared with those reported at the PDB site. For molecular docking, the three-dimensional grid box of known size (alpha amylase, size_x = 52.9921 Å, size_y = 45.6977 Å, size_z = 53.9153 Å; α-glucosidase,

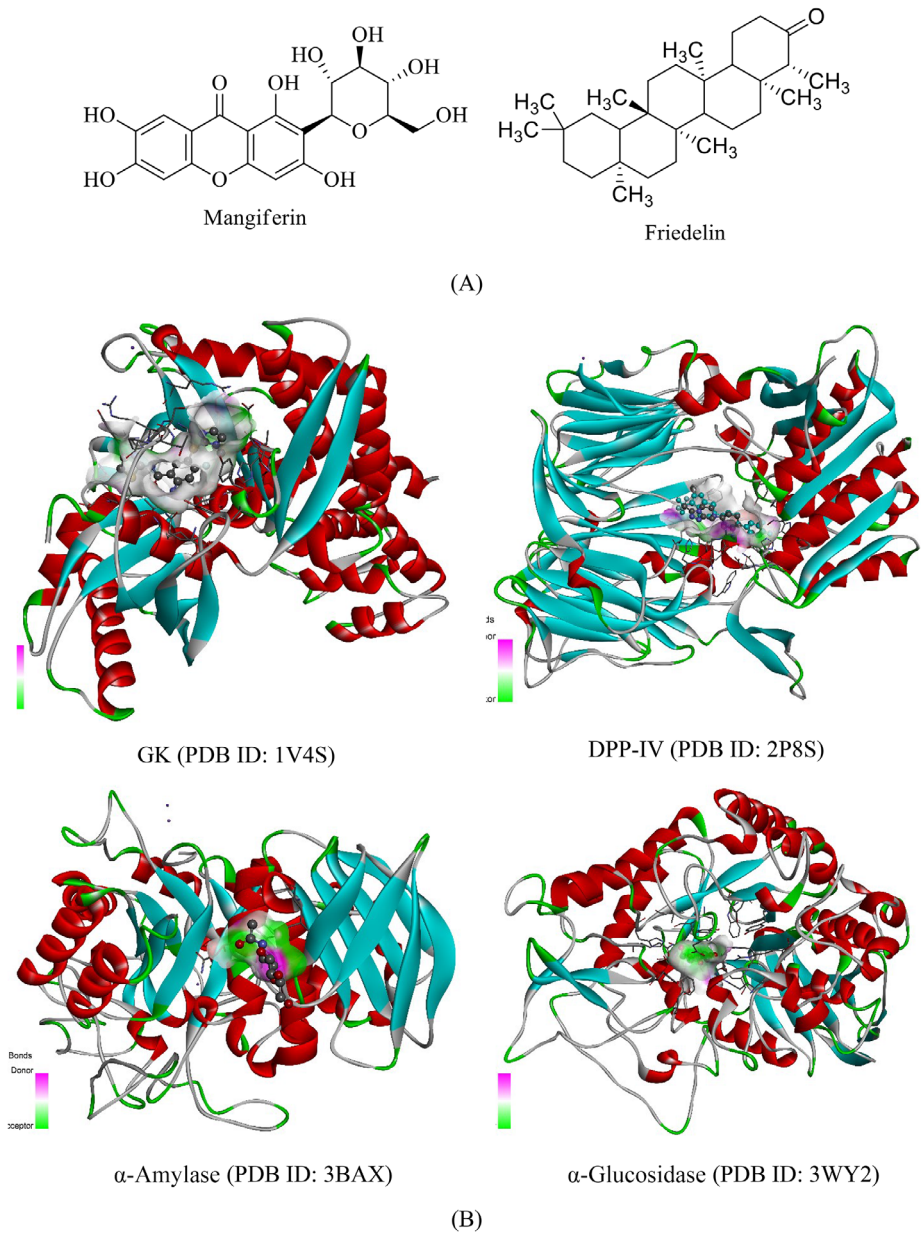

FIGURE 1 | The structures of (A) mangiferin and friedelin; (B) enzymes with native ligands in their active cavity, the same cavity has been selected for the docking of study compounds. DPP-IV, dipeptidyl peptidase-IV; GK, glucokinase; PDB, Protein Data Bank.

size_x = 52.9921 Å, size_y = 45.6977 Å, size_z = 53.9153 Å; DPP-IV, size_x = 72.5100 Å, size_y = 57.4829Å, size_z = 72.7992 Å; and GK, size_x = 51.0738 Å, size_y = 65.6269Å, size_z = 46.5124 Å) was adjusted (to define area for interactions) with an exhaustiveness value of 8. Through the use of the BIOVIA Discovery Studio Visualizer, reactive amino acid residues were discovered. Utilizing the methodology outlined by Khan et al., we were able to successfully carry out the whole molecular docking procedure, which included locating the cavity as well as the active amino acid residues [37–45]. Figure 1B depicts the structures of enzymes with native ligands in the active cavity, along with PDB codes.

2.3 | In Vitro Enzyme Assays

Mangiferin (analytical grade; CAS No.: 4773-96-0; Product No.: 06279; purity: ≥ 98.0%) and friedelin (analytical grade; CAS No.: 559-74-0; Product No.: 92187; purity: ≥ 95.0%) were obtained from Clintech Solution, Chaitanyapuri, DSNR, Hyderabad, India as gift samples for use in in vitro enzyme assays. The obtained samples were verified by determining their melting points, which were found to be consistent with the values reported in the literature. All the remaining chemicals required for the present study were purchased and procured from Lab Trading Laboratory, Aurangabad, Maharashtra, India.

2.3.1 | GK Activation Assay

The GK enzyme isolated from *Bacillus stearothermophilus* was supplied by Sigma-Aldrich as the manufacturer. After receiving enzyme assay kit, it was stored in a refrigerator at 208°C. An in vitro test was performed on the mangiferin and friedelin to see whether or not they were effective in activating GK. The

spectrophotometric method was employed to evaluate the activity of GK through a coupled reaction with glucose-6-phosphate dehydrogenase (G6PDH). GK facilitates the process of glucose phosphorylation, resulting in the production of glucose-6-phosphate (glucose-6-P). This compound is then subjected to oxidation by G6PDH, leading to the simultaneous reduction of nicotinamide adenine dinucleotide phosphate (NADPH). Subsequently, the NADPH produced is measured by tracking the augmentation in the absorption rate at 340 nm, utilizing a Shimadzu RF-6000 Fluorescence Spectrometer [46]. The molecule's activity was evaluated at a concentration of 50 μM throughout this test, known as a stimulatory concentration (SC_{50}) test. On a 96-well plate with a final reaction volume of 100 μL, a series of experiments were performed on mangiferin and friedelin with a concentration of 50 μM. The test solutions were produced by dissolving mangiferin in dimethyl sulfoxide (DMSO) and friedelin in chloroform as the respective solvents. The experiment was performed using 96-well plates. The plates had a capacity of 100 μL. They included the following components: 25 mM HEPES at a pH of 7.4, 10 mM glucose, 25 mM KCl, 1 mM $MgCl_2$, 1 mM DTT, 1 mM ATP, 1 mM NADP, 2.5 U/mL G6PDH, 1 mM glucose, 0.1 μg GK, and the chemicals being evaluated at a concentration of 50 μM. The detailed method has been performed as described by Kazi and Chatpalliwar [47] and Min et al. [48]. The SC_{50} values of mangiferin and friedelin were determined to check their GK activation potential. SC_{50} was the active efficacy of the compound stimulatory concentration of 50 μM. The activity percentage of the control group, which was not treated with GK, has been defined as 100% [46].

2.3.2 | DPP-IV Inhibition Assay

DPP-IV is the common name for the N-terminal dipeptidase serine protease. Prior to use, the enzyme assay kit was refrigerated at below 0°C. Mangiferin and friedelin were tested for their DPP-IV enzyme activity in vitro for this study. H-Gly-Pro-7-amino-4-methyl coumarin, commonly known as H-Gly-Pro-AMC, was utilized as a surrogate substrate to evaluate DPP-IV activity. Vildagliptin was used as the standard. DPP-IV cleaves the peptide link, allowing the AMC group to release. This produces fluorescence, which can be detected by spectrophotometry at a wavelength of 562 nm. The assay for DPP-IV inhibition was conducted utilizing the assay kit provided by Cayman Chemical. The serine protease DPP-IV was observed to clear the chromogenic substrate in a 96-well microtiter plate, leading to the liberation of a yellow-colored product, namely, 4-*p*-nitroaniline (*p*NA). This was achieved by quantifying the release of 4pNA from an assay mixture comprising 20 μL of DPP-IV enzyme, 0.1 M Tris–HCL buffer (pH 8.0), and varying concentrations of the test compounds, with sitagliptin as a reference. Following a 10-min incubation period, a quantity of 50 μL of substrate, specifically 2 mM Gly-Pro *p*-nitroanilide, was introduced. Subsequently, the specimens were subjected to a 30-min incubation period at a temperature of 37°C, following which the reaction was terminated by introducing sodium acetate buffer with a pH value of 4.5. The reaction mixture was kept for incubation to get enough time for the reaction of the enzyme and studied compounds to ensure proper activation or inhibition. The termination should be done to measure the effect of the compound on enzyme activity. The absorbance measurement was conducted at a wavelength of 562 nm using a microtiter plate reader. The inhibition of the DPP-IV enzyme resulted in a reduction in the formation of the yellow-colored product of DNA, accompanied by a decrease in the enzyme's activity. The activity was performed in triplicate, and the IC_{50} values were calculated [49, 50].

2.3.3 | α-Amylase and α-Glucosidase Enzyme Assay

2.3.3.1 | α-Amylase Enzyme Assay. α-Amylase and α-glucosidase enzyme assay kits were stored and refrigerated below °C before and after use. Acarbose was used as a control in this study. Mangiferin and acarbose stock solutions were prepared in an aqueous medium, whereas the friedelin stock solution was prepared using DMSO as the solvent. The solvent selected for the preparation of stock solutions was decided from the reported solubility of compounds. As friedelin is insoluble in water, DMSO was used to dissolve and prepare the stock solutions. Dinitrosalicylic acid was used to inhibit porcine α-amylase activity. A solution comprising mangiferin, friedelin, or acarbose at concentrations ranging from 02 to 16 mg/mL (100 μL) was mixed with 1 U/mL of α-amylase (100 μL) and 20 mM sodium phosphate buffer (200 μL, pH 6.9). The final concentration of the mixture ranged from 0.5 to 5.0 mg/mL. Before analysis, the specimens underwent a pre-incubation process at 25°C for 10 min. Subsequently, 200 μL of a 1% starch solution prepared in a 20 mM sodium phosphate buffer with a pH of 6.9 was introduced. The reaction mixtures underwent incubation at 25°C for 10 min. The cessation of reactions was achieved by incubating the mixture in a boiling water bath for 5 min after adding 1 mL of dinitrosalicylic acid. The mixtures undergoing reaction were subjected to cooling until they reached ambient temperature. Following this, they were diluted with water at a ratio of 1:5 and subsequently analyzed for absorbance using a Shimadzu spectrophotometer at a wavelength of 540 nm [51, 52].

2.3.3.2 | α-Glucosidase Inhibition Assay. The assessment of α-glucosidase inhibitory activity was conducted using yeast α-glucosidase and *p*-nitrophenyl-α-D-glucopyranoside (*p*NPG). Mangiferin, friedelin, or acarbose (100 μL of 02–16 mg/mL) was added to 50 μL of α-glucosidase (1 U/mL) prepared in 0.1 M phosphate buffer (pH 6.9) and 250 μL of 0.1 M phosphate buffer to get a 0.5–5.0 mg/mL final concentration. Pre-incubation of the mixture took place for 20 min. at 37°C. Following pre-incubation, a volume of 10 μL of 10 mM *p*NPG solution, prepared in 0.1 M phosphate buffer with a pH of 6.9, was introduced and subjected to incubation at a temperature of 37°C for 30 min. The cessation of reactions was achieved by introducing 650 μL of 1 M sodium carbonate, followed by the measurement of absorbance at 405 nm using a Shimadzu spectrophotometer [51, 52].

The percentage of α-glucosidase and α-amylase inhibition by mangiferin, friedelin, and acarbose was determined by using the following formula:

$$\%\ \text{inhibition} = \frac{\text{enzyme activity of control} - \text{enzyme activity of extract}}{\text{enzyme activity of control}} \times 100$$

2.4 | Molecular Dynamics Simulation (MDS)

Molecular dynamics simulation (MDS) is a computational technique used by scientists to investigate the movement and interactions of atoms and molecules, resembling a virtual experiment. Through the use of high-performance computers, scientists can replicate the actions of these minuscule particles over a duration, aiding in their comprehension of the functioning of biological systems, such as the folding of proteins or the interaction between medications and their targets. MDS is an essential tool in domains such as pharmaceutical research and materials science, facilitating scientists in making breakthroughs and resolving intricate challenges. The validation of molecular docking analysis was carried out by MDS. The Desmond module of the Schrödinger software was used to perform the MDS. Mangiferin–GK (1V4S) complex was selected to perform the MDS because mangiferin exhibited the most potent interactions with GK and formed three conventional hydrogen bonds without the development of any unfavorable hydrogen bonds. The stability of the produced complex was assessed by performing an MDS during a time period ranging from 0 to 100 ns. The orthorhombic box, with a distance of 10 Å from the borders of the box, was selected for positioning the complex using Desmond's system building module. The solvated water molecules were fixed using a predetermined model (TIP3P). The ligand associated with the 1V4S structure was rendered neutral by introducing 56 sodium (Na) ions and 36 chloride (Cl) ions, each with concentrations of 77 and 50 mM, respectively. The OPLS3e force field was used for the simulated investigation of proteins, ligands, and ions. In the molecular dynamics module, a load was chosen from a workspace with a complete system consisting of 46,305 ligand atoms with the identifier 1V4S. The simulation duration for the ongoing project was set to 100 ns to analyze the trajectories. The NPT ensemble class was chosen, whereby the temperature was held at 300K and a constant pressure of 1 atm was maintained. The assessment of many molecular dynamics characteristics was conducted, including but not limited to the root-mean-square deviation (RMSD), the protein-secondary structure element (P-SSE) graph, the root-mean-square fluctuation (RMSF) of both the protein and ligand, the analysis of complex interactions between the protein and ligand, the evaluation of long-range torsional angles (L-Torsions), and the determination of ligand properties such as polar surface area (PSA), solvent-accessible surface area (SASA), molecular surface area (molSA), and intra-molecular hydrogen bonding (IntraHB) [53, 54].

2.5 | Statistical Analysis

The experiments were conducted in triplicate ($n = 3$). The data are reported as the mean value plus or minus the standard deviation (SD). The statistical analysis was conducted using GraphPad Prism software (2365 Northside Dr. Suite 560, San Diego, CA 92108) using a one-way analysis of variance (ANOVA).

3 | Results

Table 1 lists the physicochemical properties, the drug-like characteristics, the absorption properties, metabolic profile and chemical distribution, the excretion and toxicity characteristics, an environmental toxicity profile (bioconcentration factors: IGC_{50}, $LC_{50}FM$, and $LC_{50}DM$) calculated for mangiferin and friedelin in comparison to the co-crystallized ligands (CCLs). The binding poses of the molecules are depicted in Figure 2A–D. The DPP-IV enzyme assay results are tabulated in Table S3, and the graph is depicted in Figure 3A. The activity results of α-amylase and α-glucosidase inhibition assay are tabulated in Table S4, and graphs are depicted in Figure 3B,C. The RMSD outcomes for the ligand and ligand–complex system in conjunction with 1V4S are shown in Figure 4A.

4 | Discussion

4.1 | In Silico Drug-Like Profile

Novel medications rely significantly on chemical absorption, distribution, metabolism, and excretion processes, together known as ADME, for their discovery and development. An optimal medication candidate must possess enough efficacy against the therapeutic target and superior ADME characteristics at the therapeutic dosage. An analysis was conducted to assess the toxicity, drug-likeness, and ADME profiles of the compound. A unique approach, known as in silico ADMET assessment models, has been created to further support medicinal chemists in creating and improving leads. Pharmacokinetic qualities enable researchers to examine the biological impacts of potential pharmaceutical candidates. Pharmacokinetic qualities play a vital role in the development of novel medications [42]. All of the molecular weights (MW), hydrogen acceptors (nHAs), hydrogen donors (nHDs), rotatable bonds (nRots), van der Waals (vdW) volumes, and total PSAs (TPSAs) were within the allowable range in the physicochemical analysis. As shown by its logP and logS values, the drug's lipophilicity is crucial in several pharmacokinetic properties, such as solubility, absorption, membrane permeability, plasma protein binding (PPB), distribution, and tissue penetration. Due to the significant relevance of the drug's lipophilicity, the Lipinski rule of five has been updated to include both logP and logS. All of these parameters were determined to fall within the suitable range and exhibited optimal oral bioavailability in the present investigation, indicating that they might be adapted for administration via the oral route [55, 56].

Several parameters, including the quantitative estimate of drug-likeness (QED), the natural product-likeness score (NPscore), the Lipinski rule, the Pfizer rule, the GSK rule, the Golden Triangle, and the Chelator rule, were determined. The QED, introduced in 2012, is a metric for determining drug-likeness. It is a measure of drug-likeness that is constructed utilizing data from existing medications on the market. In modern times, computational tools and evaluations of drug-like characteristics are widely used in creating small-molecule medications. The majority of the compounds, including mangiferin, friedelin, and CCLs, had favorable QED values [57, 58]. In most cases, the NP score is between −5 and 5. For a given molecule, a higher score indicates a higher probability that it is an NP [59, 60]. Within this range, both mangiferin and friedelin exhibited NP-like characteristics. According to the Pfizer rule, substances that have a log p value more than 3 and a TPSA value lower than 75 are likely to exhibit toxicity [61]. As per the GSK rule, molecules

TABLE 1 | ADMET profiles calculated for mangiferin, friedelin, and co-crystallized ligands (CCLs).

Lipinski rule of 5 and Veber's rule								
Compound	**Physicochemical property**							
	Molecular weight	**Volume**	**nHA**	**nHD**	**nRot**	**TPSA**	**logS**	**logP**
MRK (1v4s)	349.50	310.799	6	3	4	89.060	−3.050	2.288
Cyclohexalamine derivative (2p8s)	419.150	363.865	5	2	3	59.970	−1.211	1.409
NAG (3bax)	221.090	199.470	7	5	3	119.250	−0.151	−1.931
Glucose (3wy2)	180.060	156.517	6	5	1	110.380	−0.093	−2.101
Mangiferin	422.080	381.192	11	8	2	201.280	−3.514	0.136
Friedelin	426.390	490.807	1	0	0	17.070	−6.442	6.880

Drug-likeness properties							
	Medicinal chemistry						
	QED	**NPscore**	**Lipinski rule**	**Pfizer rule**	**GSK rule**	**Golden Triangle**	**Chelator rule**
MRK (1v4s)	0.711	−2.279	Accepted	Accepted	Accepted	Accepted	0 alert
Cyclohexalamine derivative (2p8s)	0.600	−0.766	Accepted	Accepted	Rejected	Accepted	0 alert
NAG (3bax)	0.337	2.019	Accepted	Accepted	Accepted	Accepted	0 alert
Glucose (3wy2)	0.290	2.627	Accepted	Accepted	Accepted	Rejected	0 alert
Mangiferin	0.191	1.999	Rejected	Accepted	Rejected	Accepted	1 alert
Friedelin	0.379	2.644	Accepted	Rejected	Rejected	Rejected	0 alert

Absorption parameters							
	Absorption						
	Caco-2 permeability	**MDCK permeability**	**Pgp-inhibitor**	**Pgp-substrate**	**HIA**	**F20%**	**F30%**
MRK (1v4s)	−4.358	2.8e − 05	−−	−−	−	−	−
Cyclohexalamine derivative (2p8s)	−5.036	1.5e − 05	−−	−−	−	−	−
NAG (3bax)	−5.327	9.6e − 05	−−	++	++	−	++
Glucose (3wy2)	−5.390	0.00032	−−	−	++	−	++
Mangiferin	−6.286	4.5e − 06	−−	+++	++	++	++

(Continues)

TABLE 1 | (Continued)

Absorption parameters																
					Absorption											
					Caco-2 permeability		MDCK permeability		Pgp-inhibitor		Pgp-substrate		HIA		F20%	F30%
Friedelin					−5.092		7.2e − 06		−		−−		−		++	++
Distribution and metabolism profile																
	Distribution				Metabolism											
	PPB (%)	VD	BBB penetration	Fu (%)	CYP1A2		CYP2C19		CYP2C9		CYP2D6		CYP3A4			
					Inhibitor	Substrate	Inhibitor	Substrate	Inhibitor	Substrate	Inhibitor	Substrate	Inhibitor	Substrate		
MRK (1v4s)	69.0	1.1	+++	32.0	+++	+	+++	−	+	++	−−	+	+	−		
Cyclohexalamine derivative (2p8s)	54.7	3.8	−	44.8	−−	−−	−	++	−	−	++	+	++	−		
NAG (3bax)	12.8	0.4	−	87.7	−−	−−	−−	−−	−−	−−	−−	−−	−−	−−		
Glucose (3wy2)	13.6	0.4	−	79.7	−−	−−	−−	−	−−	−	−−	−	−−	−−		
Mangiferin	85.7	0.9	−−	21.9	−	−	−	−	−	−	−	−	−	−		
Friedelin	97.7	1.6	++	2.19	−−	+	−−	+++	−−	−	−−	−	−	++		
Excretion and toxicity profile																
	Excretion		Toxicity													
	CL	T1/2	H-HT	DILI	AMES toxicity	Rat oral acute toxicity	FDAMDD	Skin sensitization	Carcinogenicity	Eye corrosion	Eye irritation	Respiratory toxicity				
MRK (1v4s)	6.091	0.260	+++	+++	+++	−	+++	−	++	−−	−−	+++				
Cyclohexalamine derivative (2p8s)	7.250	0.279	+++	−	−−	+	+++	−	+	−−	−−	++				
NAG (3bax)	1.803	0.819	−	−	+	−−	−−	−−	−−	−−	−−	−−				
Glucose (3wy2)	1.602	0.821	−−	−−	−	−−	−−	−	−−	−−	++	−−				
Mangiferin	3.792	0.868	−	+++	++	−−	−−	+++	−−	−−	++	−−				
Friedelin	16.265	0.037	−	−	−−	−	−	−	−−	−	−−	+++				

(Continues)

TABLE 1 | (Continued)

Compound	Environmental toxicity profile			
	Environmental toxicity			
	Bio-concentration factors	IGC_{50}	$LC_{50}FM$	$LC_{50}DM$
MRK (1v4s)	0.635	3.825	3.952	4.896
Cyclohexalamine derivative (2p8s)	1.962	2.751	3.581	7.350
NAG (3bax)	0.271	0.522	0.918	1.100
Glucose (3wy2)	0.263	0.925	0.913	2.102
Mangiferin	0.981	4.045	4.728	5.513
Friedelin	1.749	5.184	5.785	6.673

Note: Here, Pgp-inhibitor/substrate: −−, +++, strong; −, ++, moderate; −, +, low. In HIA, ++, HIA <30%; −, HIA ≥30%. In F20% and F30%; ++, bioavailability < 20% and 30%, respectively; −, bioavailability ≥ 20% and 30%, respectively; −−, +++, strong; −, ++, moderate; −, +, low.

Abbreviations: nHA, hydrogen acceptor; nHD, hydrogen donor; nRot, rotatable bond; TPSA, total polar surface areas; HIA, intestine absorption in humans; PPB, plasma protein binding; VD, volume distribution; BBB, blood–brain barrier.

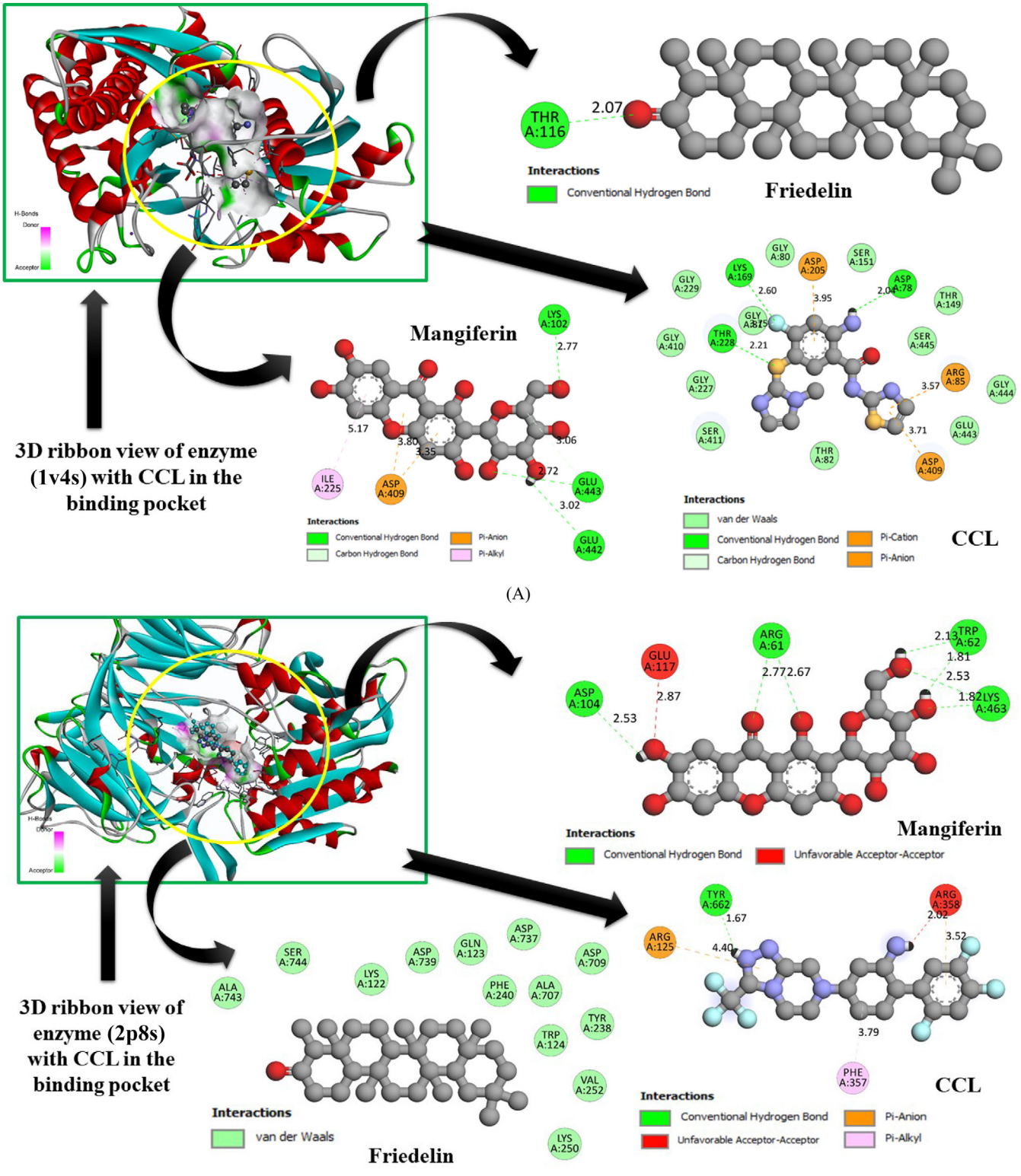

FIGURE 2 | The binding poses of molecules with enzymes: (A) MRK, mangiferin, and friedelin with glucokinase enzyme; (B) cyclohexalamine derivative, mangiferin, and friedelin with DPP-IV enzyme; (C) NAG, mangiferin, and friedelin with α-amylase enzyme; (D) NL, mangiferin, and friedelin with α-glucosidase enzyme. CCL, co-crystallized ligand.

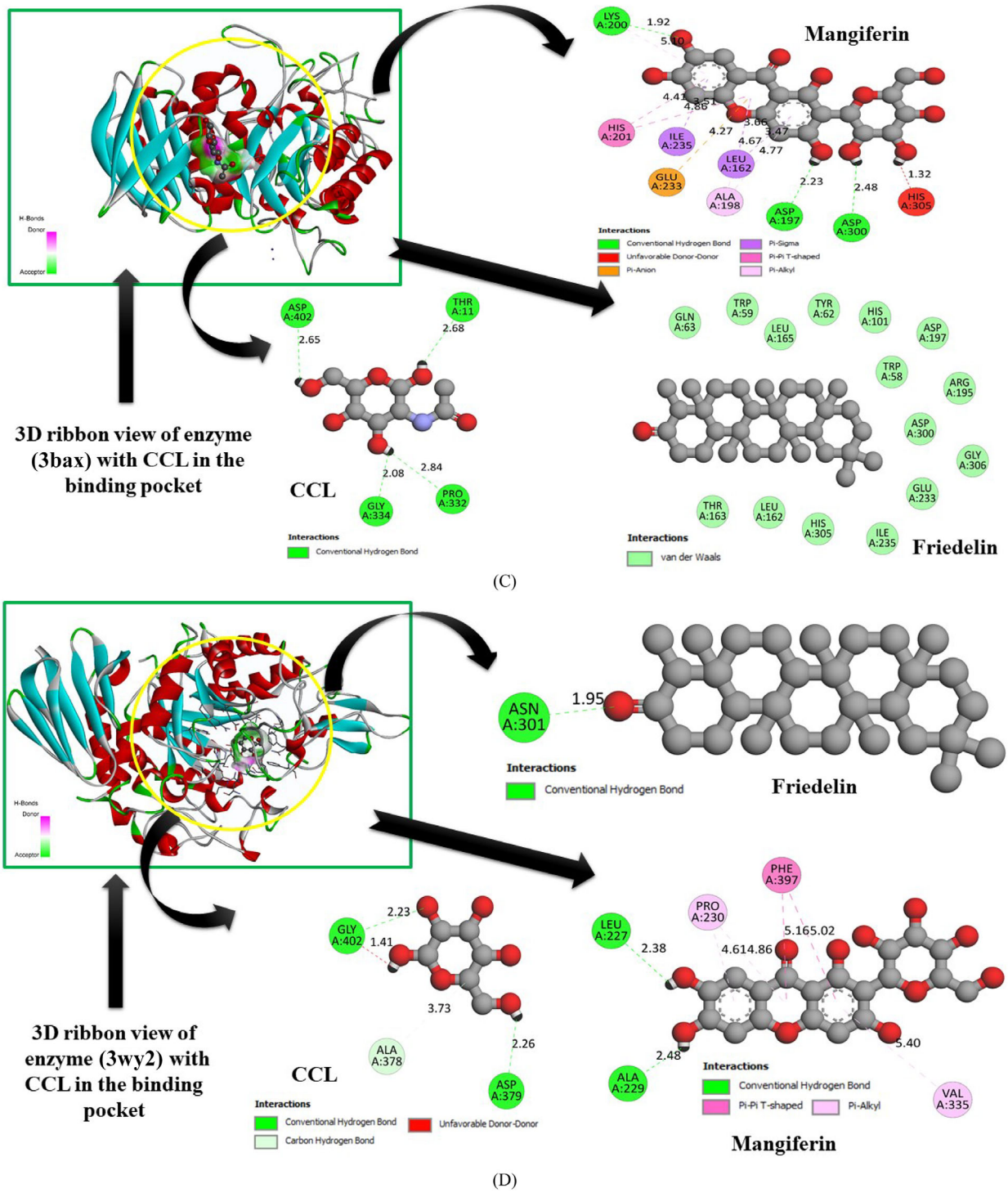

FIGURE 2 | (Continued)

having a molecular mass below 400 and a CLogP below 4 are more likely to have an ideal ADME profile [62]. Using in vitro permeability, in vitro clearance, and computational data, the Golden Triangle ($200 \leq MW \leq 50$; $-2 \leq logD \leq 5$) was created as a visualization tool to help medicinal chemists discover drug candidates that are metabolically stable, permeable, and powerful [63]. Only the CCLs of 1v4s, 3bax, and 3wy2 conformed to the GSK rule, even though molecules meeting the criteria may have a superior ADMET profile. Compounds that adhere to the Golden Triangle concept can demonstrate an improved ADMET profile.

Absorption parameters play a crucial role in drug development because they provide valuable information on how much a medicine enters the bloodstream after administration. Through comprehension of these criteria, such as the solubility and intestinal permeability of a medicine, scientists may make predictions about the efficacy of a treatment inside the human body. Enhancing these absorption coefficients may ensure that medications are more likely to exhibit efficacy and safety when administered. The Caco-2 cell line, derived from human colon epithelial carcinoma, is a representative model for studying

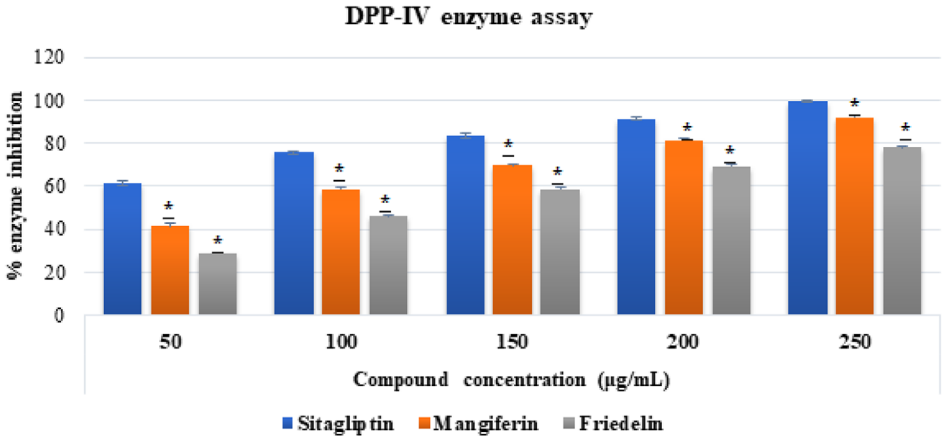

(A)

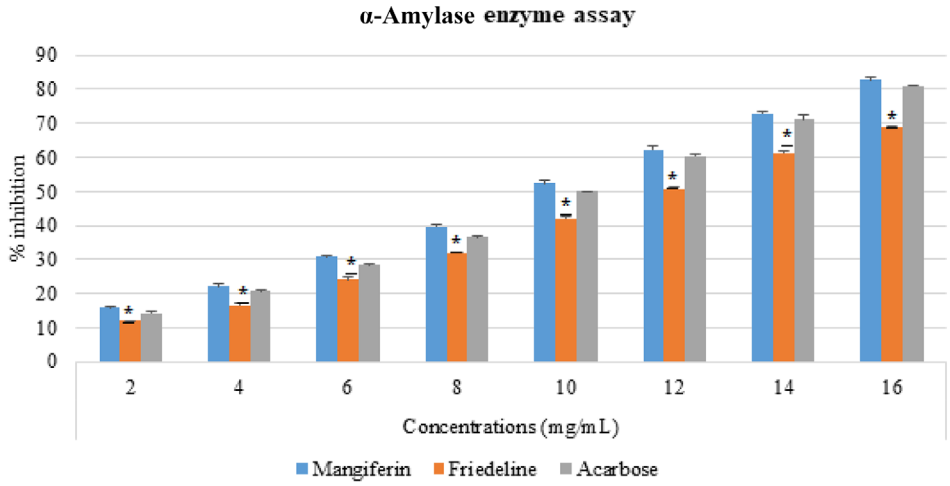

(B)

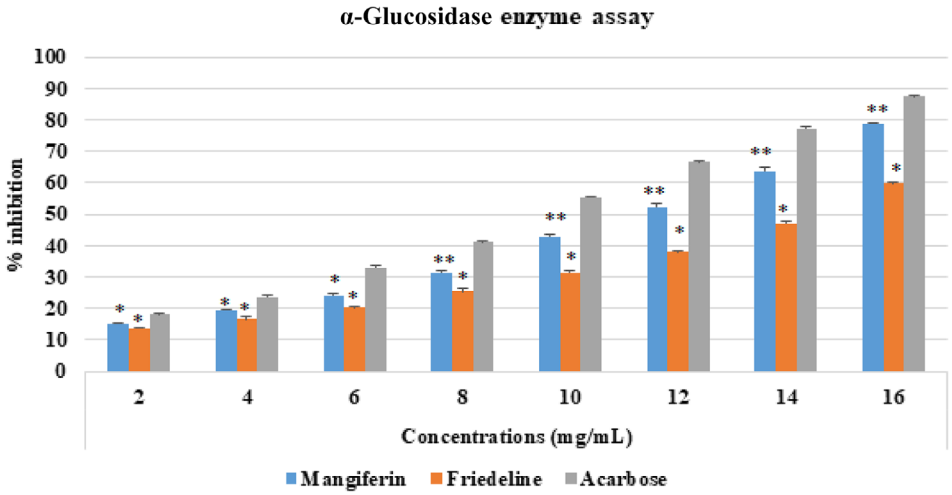

(C)

FIGURE 3 | In vitro enzyme assays of mangiferin and friedelin: (A) graph of DPP-IV enzyme assay; (B) graph of α-amylase enzyme assay; (C) graph of α-glucosidase enzyme assay. The values are expressed as mean ± SD ($n = 3$). The data were statistically analyzed by one-way ANOVA followed by Dunnett's post hoc test. Graph showed that sitagliptin versus mangiferin and friedelin = $^{*}p < 0.05$; acarbose versus mangiferin and friedelin = $^{*}p < 0.05$; acarbose versus mangiferin and friedelin = $^{*}p < 0.05$ and $^{**}p < 0.01$. DPP-IV, dipeptidyl peptidase-IV.

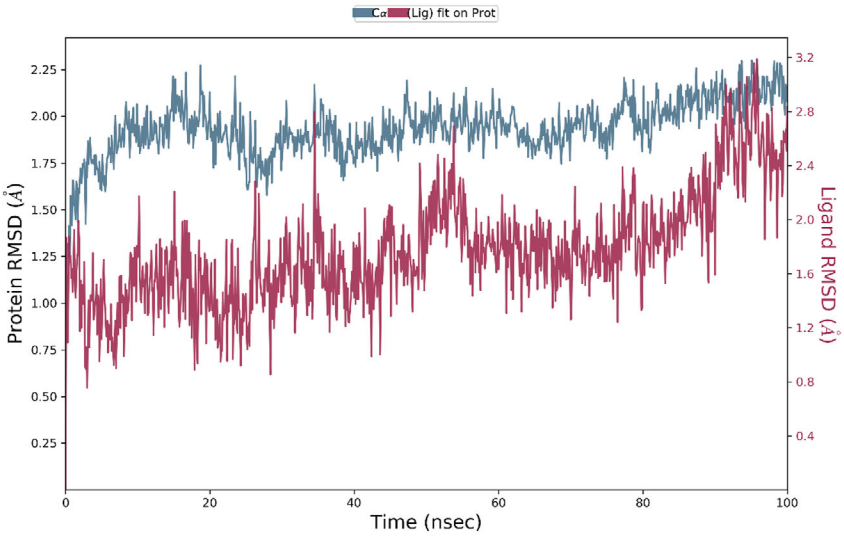

(A)

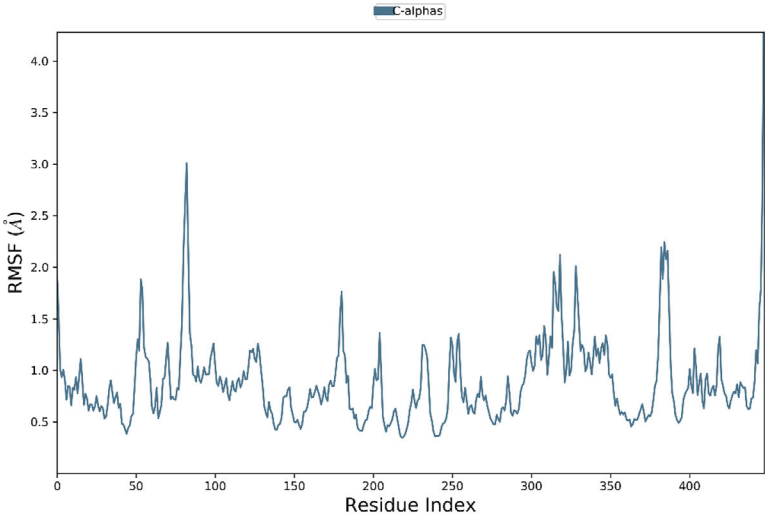

(B)

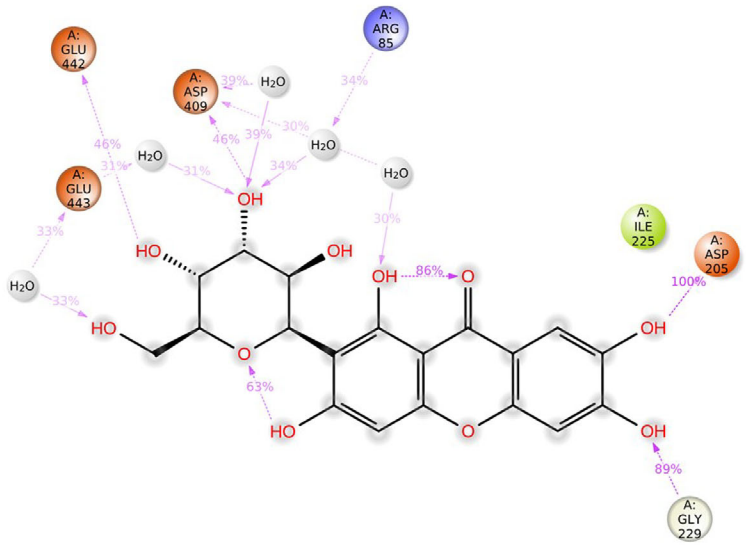

(C)

FIGURE 4 | The molecular dynamics results: (A) protein–ligand interactions in RMSD; (B) the RMSF plot of protein; (C) 2D plot of mangiferin with GK (1V4S). RMSD, root-mean-square deviation; RMSF, root-mean-square fluctuation.

medication absorption throughout the digestive system. Intestinal permeability predictions and drug efflux studies may both benefit from this approach. It was observed that every single compound exhibited the highest possible Caco-2 permeability, which is attained when the value is more significant than −4.358 log unit [64]. Researchers can better understand medication efflux with the assistance of MDCK-MDR1, which also shows early warning indications of drug permeability concerns. It was shown that the permeability of MDCK-MDR1 is a good predictor of the permeability of the blood–brain barrier (BBB), which is a barrier that complements the permeability of the intestinal barrier [65]. Several of the compounds exhibited Pgp-substrate and Pgp-inhibitor activities. Mangiferin and the CCLs of 3bax and 3wy2 showed good intestine absorption in humans (HIA). F20% and F30% bioavailability of the molecules, mangiferin and friedelin, were within the range of acceptable values [35].

Several compounds showed PPB (<90%) of less than 90%, suggesting that medicines with high protein binding may have a poor therapeutic index. All the compounds had a volume distribution (VD, optimum 0.04–20 L/kg) within acceptable limits. The BBB is a specialized system of brain microvascular endothelial cells (BMVECs) that serves to protect the brain from toxic substances present in the bloodstream while simultaneously providing essential nutrients to brain tissues. Additionally, the BBB filters out harmful compounds from the brain and returns them to the bloodstream. The passage of substances across the BBB is tightly regulated by physical factors, such as tight junctions and metabolic barriers, which consist of enzymes and other transport mechanisms. The BBB presents a substantial obstacle to delivering therapeutic medicines to the CNS because of its limited permeability [66]. Only friedelin and MRK displayed BBB penetration potential. Being a substrate or inhibitor of a cytochrome enzyme adds to drug activity because of its function in drug metabolism [43, 67]. In the present investigation, the CCLs of 1v4s showed CYP1A2, CYP2C19, CYP2C9, CYP2D6, and CYP3A4 inhibition, while friedelin showed substrate potential [35].

Gaining knowledge about the elimination of medications from the body and their capacity to induce damage is crucial in the field of drug research. Excretion profiles elucidate the duration of drug presence in the body and the mechanisms by which it is eliminated, thus influencing the frequency of administration and the potential for accumulation. Toxicity profiles assist in determining if a medicine may elicit any detrimental effects on the body, such as side effects or responses. By conducting early studies on these characteristics, scientists may prioritize developing safer and more efficacious pharmaceuticals, which is advantageous for patients who depend on these prescriptions. Except for friedelin, all the compounds had a clearance rate ranging from low to moderate. A high clearance rate, over 15 mL/min/kg, was seen only for friedelin, which showed a clearance rate of 16.265 mL/min/kg. All the molecules had a brief half-life, with a $T_{1/2}$ of less than 3 h. The toxicity profile of the recommended compounds exhibited favorable characteristics, with several values falling below the acceptable range. Except for MRK and cyclohexylamine, none of the compounds exhibited human hepatotoxicity. Drug-induced liver injury was seen in mangiferin and MRK. The Ames assay is a standard and reliable technique for testing chemical mutagens for their ability to rescue mutant *Salmonella typhimurium* and/or *Escherichia coli* bacteria from their inability to produce amino acids. The bacterial reverse mutation assay is another name for this technique [68]. In this investigation, mangiferin displayed Ames toxicity, indicating its mutagenic properties. Maximum recommended daily dose, Ames toxicity, and rat oral acute toxicity were shown with MRK and cyclohexalamine derivative. Carcinogencity was shown by MRK and cyclohexalamine derivatives, whereas respiratory toxicity was shown by MRK, cyclohexalamine derivatives, and friedelin. Figure S1 presents the physicochemical profile of the compounds obtained from the ADMETlab 2.0 web server. This profile highlights the desirable physicochemical properties of the molecules, which may guide their future development [35]. These are the at-a-glance drug-like properties of all the molecules discussed in the above section.

It is crucial to evaluate their environmental toxicity profile during drug development to understand how chemicals may affect ecosystems and their surrounding habitats. By looking at a chemical's biodegradability, bioaccumulation, and ecotoxicity, scientists may predict how dangerous it may be to aquatic life, other animals, and ecosystems. Understanding the environmental toxicity profile early on in the drug development process can detect and mitigate environmental risks, leading to sustainable pharmaceuticals that are safe for humans and the planet. The utilization of bioconcentration factors is crucial in assessing the risks to human health associated with the food chain, particularly the potential for secondary poisoning. The bioconcentration factor is measured in $-\log10[(mg/L)/(1000 \times MW)]$ [69, 70]. Cyclohexalamine derivative and friedelin displayed a higher bioconcentration factor than MRK, NAG, glucose, and mangiferin. The toxicity of various compounds was assessed using *Tetrahymena pyriformis* as the test subject. The IGC_{50}, which stands for the concentration causing 50% growth inhibition in *T. pyriformis*, was utilized in this experiment. The LC_{50}FM, which pertains to the acute toxicity (96-h LC_{50}) of 397 distinct organic compounds to the fathead minnow (FM), has been established by implementing a group contribution methodology [71]. *Daphnia magna*, commonly called *D. magna*, is a model bioindicator in ecotoxicology due to its remarkable susceptibility to pollutants. The LC_{50}DM is the concentration at which 50% of the Daphnia in a test batch becomes immobilized during a continuous exposure period, which usually lasts for 48 h [72]. The compounds' environmental toxicity profiles were ideal or at least below tolerable limits.

4.2 | Molecular Docking

Researchers use molecular docking to better understand how possible medications may function in the body, which is analogous to a computer simulation. Predicting how well a drug candidate will bind to its target protein is crucial for ensuring its efficacy. Molecular docking allows investigators to develop novel medications more quickly while improving their efficacy and safety. Molecular docking helps screen virtually all compounds to ascertain the ligand's potential activity against biological targets. The molecular interactions of the compounds mentioned in the title are shown in Table S1. The following part discusses the binding affinities of the compounds under investigation with the enzymes possessing crystal structures 1v4s, 2ps8, 3bax, and 3wy2.

4.2.1 | Glucokinase

The re-docking of the CCL MRK of 1v4s was performed to ascertain the scoring function. MRK displayed a docking score of −7.2 kcal/mol and established three conventional hydrogen bonds with Asp78, Lys169, and Thr228 in addition to one carbon–hydrogen bond with Thr228. It established many electrostatic interactions, such as Pi–cation and Pi–anion bonds with Arg85, Asp205, and Asp409. Mangiferin showed a docking score of −8.3 kcal/mol, and it established three conventional hydrogen bonds with Glu442, Lys102, and Glu443 in addition to one carbon–hydrogen bond with Glu443. It has established a large number of electrostatic interactions, such as Pi–anion bonds with Asp409 and hydrophobic (Pi–alkyl) types of interactions with Ile225. Friedelin exhibited a docking score of −8 kcal/mol and formed only one conventional hydrogen bond with Thr116. Mangiferin and friedelin displayed more binding potential than CCLs with the GK enzyme. It could be submitted to an in vitro test to evaluate the inhibitory activity.

4.2.2 | DPP-IV

DPP-IV inhibitors are crucial for controlling T2DM because they improve glucose regulation. These medications inhibit the enzyme DPP-IV, which has a role in controlling blood sugar levels. The medication for diabetes works by inhibiting DPP-IV, impeding the degradation of incretin hormones. These hormones subsequently decrease blood sugar levels by promoting insulin synthesis and inhibiting glucagon release. DPP-IV inhibitors are often included in comprehensive treatment programs for T2DM to regulate blood sugar levels effectively, reduce hemoglobin A1c levels, and avoid the risk of hypoglycemia or weight gain. The re-docking of the CCL cyclohexalamine derivative of 2p8s was performed. The cyclohexalamine derivative displayed a docking score of −9.1 kcal/mol and formed one conventional hydrogen bond with Tyr662. It has established electrostatic interactions, such as Pi–cation bonds with Arg125 and Arg358 and hydrophobic (Pi–alkyl) interactions with Arg358 and Phe357. Mangiferin exhibited a docking score of −7.9 kcal/mol and formed seven conventional hydrogen bonds with Trp62, Asp104, Arg61, and Lys463. Friedelin showed a docking score of −9.5 kcal/mol and showed vdW force of attraction with Ala743, Ser744, Lys122, Asp739, Gln123, Asp737, Phe240, Ala707, Tyr124, Tyr238, and Val252. Friedelin showed a higher binding potential than the CCL, and it could be submitted to in vitro tests. Mangiferin showed a lower binding potential than the cyclohexalamine derivative. Still, the close values suggest submitting mangiferin to in vitro tests, considering that in vitro activity is not always strictly related to docking score [73].

4.2.3 | α-Amylase

The re-docking of the CCL NAG of 3bax was performed. NAG displayed a docking score of −5.7 kcal/mol and formed four conventional hydrogen bonds with Thr11, Pro332, Gly334, and Asp402. Mangiferin showed a docking score of −9.3 kcal/mol, generating three conventional hydrogen bonds with Asp300, Asp197, and Lys200. It established many hydrophobic interactions (Pi–anion, Pi–sigma, Pi–Pi T-shaped, and Pi–alkyl) with Leu162, Ile235, His201, Ala98, and Lys200. Friedelin showed vdW force of attraction with Gln63, Trp59, Leu165, Tyr62, His101, Asp197, Arg195, Asp300, Gly306, Glu233, Ile2235, His305, Leu162, and Thr163, along with a docking score of −10.7 kcal/mol. It was observed that both mangiferin and friedelin have a higher docking score than the CCL NAG, and they could be tested in vitro as α-amylase inhibitors and developed further.

4.2.4 | α-Glucosidase

The re-docking of the CCL Glucose of 3wy2 was performed. Glucose displayed a docking score of −5.6 kcal/mol, and it established two conventional hydrogen bonds with Asp379 and Gly402 in addition to one carbon–hydrogen bond with Ala378. Mangiferin showed a docking score of −8.2 kcal/mol, generating three conventional hydrogen bonds with Leu227 and Ala229. It established many hydrophobic interactions (Pi–Pi T-shaped, Pi-alkyl) with Phe397, Pro230, and Val335. Friedelin exhibited a docking score of −8.8 kcal/mol and formed one conventional hydrogen bond with Asn301. It was observed that both mangiferin and friedelin have a higher docking score than the CCL glucose and they could be tested in vitro as α-glucosidase inhibitors.

4.3 | In Vitro Enzymatic Assays

Molecular docking studies showed that mangiferin and friedelin displayed encouraging binding potential with all the enzymes and can cause significant conformational changes in the enzyme to modulate their activities. Even though it was observed that mangiferin violated the drug-likeness rule, there is evidence that nanoformulations containing mangiferin displayed better drug absorption and potency [74, 75]. Given these findings, we performed in vitro enzymatic assays on the four enzymes and the two natural compounds.

4.3.1 | GK Activation Assay

The GK plays a crucial part in the body's ability to detect elevated blood glucose levels. The pancreas uses it as a "glucose sensor," causing more insulin to be secreted in response to rising blood sugar levels. In structure-based virtual ligand screening, mangiferin has been singled out as a compound with GK activator properties [76]. Enzyme activation experiments and in vitro cell-based tests confirmed its micromolar range potency. The antihyperglycemic action of this drug was shown in db/db mice without the occurrence of any adverse consequences, such as hypoglycemia [48]. Sunil et al. examined friedelin's (a compound isolated from *Azima tetracantha* leaves) antidiabetic effect by probing its molecular basis. For 28 days, diabetic rats caused by streptozotocin (STZ) were given friedelin at 20 and 40 mg/kg. Changes in body mass index (BMI), blood glucose, insulin, SGOT, SGPT, SALP, liver glycogen, and total protein were measured after 28 days of therapy. As a result of taking friedelin, these abnormal levels returned to within the normal range. Friedelin increased GLUT2 and GLUT4 translocation and activation in skeletal muscle and liver of diabetic rats through the PI3K/p-Akt signaling cascade [32]. The GK activation potential of mangiferin and friedelin was investigated in the present study, and both displayed significant activities. Mangiferin displayed

120.1% ± 1.84% GK activation at 50 μg/mL concentrations, whereas friedelin displayed 105.4% ± 1.82% activation, which means no significant activation of GK by friedelin. Blank was considered the control in this experiment with 100% GK activity. Mangiferin and friedelin could be a starting point for developing more potent GK activators.

4.3.2 | DPP-IV Inhibition Assay

All known DPP-IV inhibitors are tiny compounds that selectively block the enzyme's catalytic activity without impacting the protein's other known activities. The majority of patients with T2DM find DPP-IV inhibitors to be safe and effective. This is because of the drugs' favorable therapeutic profile and the fact that they have been shown not to raise cardiovascular risk [77]. The preventative benefits of mangiferin on many parameters of metabolic syndrome, including diabetes, were studied by Suman et al. [78]. Mangiferin therapy improved many symptoms of metabolic syndrome, including dyslipidemia and insulin sensitivity. Furthermore, when comparing the mangiferin-treated group to the high-fat diabetic control group, the former showed elevated blood insulin and C-peptide levels and a decreased homeostasis model evaluation-β of insulin resistance-IR. Furthermore, mangiferin was revealed to have cardioprotective properties. Serum DPP-IV levels decreased in the mangiferin group, linked with better insulin resistance and increased β-cell function. Results from the above research show that mangiferin has antidiabetic, hypolipidemic, and cardioprotective effects in the context of diabetes with metabolic syndrome. Because of its potential usefulness in treating this comorbid illness, mangiferin may one day serve as a natural substitute for synthetic DPP-IV inhibitors [78]. In the present study, mangiferin and friedelin demonstrated 74.93 ± 0.71 and 110.64 ± 0.21 μg/mL of IC_{50} values, respectively. Sitagliptin was standard, which showed 44.76 ± 0.53 μg/mL of IC_{50} value.

4.3.3 | α-Amylase and α-Glucosidase Inhibition Assay

α-Amylase, a digestive enzyme largely present in saliva and pancreatic juice, is critically significant due to its function in the breakdown of polysaccharides. An enzyme that plays a role in glucose production after meals might be targeted and inhibited to lower blood sugar levels after meals. One of the most important digestive enzymes, α-glucosidase is found in the mucosal brush border of the small intestine. It breaks down complicated carbs into more manageable forms that the body can use. Delaying glucose absorption and avoiding high postprandial blood glucose levels by their suppression is a promising strategy for potentially slowing the course of diabetes [79]. In vitro enzyme assays of mangiferin and friedelin were performed, and significant inhibitions with optimum potency have been observed. Inhibitors of α-glucosidase and α-amylase, such as acarbose, are often used for treating T2DM. Acarbose is a complex oligosaccharide that inhibits and slows the intestinal absorption of glucose, hence lowering the postprandial increase of blood glucose levels in T2DM [80]. Therefore, in the present investigation, acarbose was used as the standard. Against α-amylase enzyme, mangiferin, friedelin, and acarbose demonstrated 9.72 ± 0.15, 11.84 ± 0.06, and 10.19 ± 0.05 mg/mL of IC_{50} values, respectively. In α-glucosidase enzyme assay, mangiferin, friedelin, and acarbose displayed 11.72 ± 0.10, 14.34 ± 0.02, and 9.14 ± 0.06 mg/mL of IC_{50} values, respectively. It was observed that mangiferin and friedelin were both more potent as α-amylase inhibitors than α-glucosidase.

4.4 | MDS Results

The use of the Desmond module in conducting MDS has provided empirical evidence supporting the stability and reliability of compounds that have effectively achieved target binding. MDS were conducted using simulation intervals of 100 ns. The stability of a complex was assessed by calculating the RMSD and RMSF. These metrics were used to confirm the findings obtained from docking scores. The RMSD was used to assess the interactions between a drug and a target. The calculation of RMSD included the careful selection of atoms. The RMSD analysis assessed the structural confirmation of both ligands and proteins. The RMSD analysis indicates that the ligand and ligand–complex system exhibited stability while interacting with enzyme 1v4s. Examining the ligand and ligand–complex system using the RMSD method revealed a high level of stability, with no observed deviations during the simulation period. The complex stability throughout the simulation period should ideally be maintained below a threshold of 3 Å. The ligand complex's RMSD was determined to range from 1 to 2 Å, indicating a consistently stable conformation throughout the simulation.

This study aims to analyze the RMSF trajectory to assess the mobility of molecules about ligand binding and local alterations within protein chains. Using protein RMSF, the analysis of fluctuation and positional disparities of alpha-carbon atoms was conducted. The investigation of the ligand–complex system revealed a noteworthy observation in the RMSF of the alpha carbon. No changes were observed in the RMSF of the protein, as shown in Figure 4B.

The present study demonstrates that these interactions exhibit significant strength when the proportion of amino acids involved in contacts exceeds 30.0%. This observation is based on the analysis of simulation data obtained from the chosen trajectory, which spans a time period of 0–100 ns. The ligand associated with the 1v4s protein structure had a robust interaction with ASP205, with a 100% occurrence rate, representing the most pronounced interactions observed. Furthermore, it is worth noting that many additional amino acids have shown notable interactions. For instance, GLY229 has demonstrated interactions with a frequency of 89%. Similarly, ASP409 and GLU442 have displayed interactions with a frequency of 46%. Additionally, ARG85 has shown interactions with a frequency of 34%. Moreover, there have been observations of weak interactions, accounting for around 30% of the total interactions, as seen in Figure 4C.

The properties of ligands are evaluated using different parameters such as the radius of gyration (rGyr), the number of internal hydrogen bonds (IntraHB), the surface area of the molecule (MolSA), the surface area accessible to solvent (SASA), and the PSA, which are analyzed using Desmond simulation. The rGyr is a critical parameter in the field of drug development because it provides a quantitative measure of the flexibility and conformational changes exhibited by molecules. This information is invaluable in optimizing ligand binding and designing effective

drugs. Through the evaluation of rGyr, scientists can choose ligands that possess ideal structural characteristics for efficient interactions with certain proteins, creating more powerful and specific drugs. The rGyr is highly important as it quantifies the ligand's degree of flexibility and spatial arrangement. During the simulation, the protein's average radius remains constant. Protein compression is apparent as the gyration radius decreases during the simulation, whereas an increase suggests the opposite effect. The simulation results of the ligand–complex system indicate a significant degree of stability within the protein's binding pocket.

5 | Conclusions

A wide variety of compounds derived from herbal sources have been shown to have several applications in the fields of general biology, pharmacy, and medicine. The present study aimed to examine the inhibitory capacity of mangiferin and friedelin on various enzymes, namely, GK, DPP-IV, α-amylase, and α-glucosidase, through a computer-aided drug design methodology. This was followed by a comprehensive analysis of ADMET and in vitro enzyme assays. These compounds showed encouraging in silico ADMET and drug-likeness properties. Molecular docking studies showed that mangiferin and friedelin had potential binding affinities with all the enzymes. The molecular dynamic study also revealed remarkable changes and showed the ligand–complex stability, which means the mangiferin and protein binding is good enough. This evidence was exploited to perform in vitro enzymatic assays in which mangiferin and friedelin were shown to activate GK 20% and 5% more than the basal activity of the enzyme. Mangiferin and friedelin demonstrated significant IC_{50} values in the DPP-IV enzyme assay and good inhibitory potential. Moreover, mangiferin and friedelin showed IC_{50} values comparable to acarbose in α-amylase and α-glucosidase enzyme assays. The present study's findings suggest that mangiferin and friedelin have potential for therapeutic development in T2DM. Before implementation, it is imperative to generate substantial clinical evidence from diverse in vivo and in vitro models.

Author Contributions

Ravikiran Maheshrao Suryawanshi: conceptualization, data curation, formal analysis, investigation, methodology, resources, software, supervision, visualization, roles/writing–original draft, writing–review and editing. **Rupali Bhalchandra Shimpi**: data curation, investigation, methodology, resources, software, roles/writing–original draft, writing–review and editing. **V. Muralidharan**: data curation, investigation, methodology, resources software, roles/writing–original draft, writing–review and editing. **Lalita Shashikant Nemade**: data curation, investigation, methodology, resources, software, roles/writing–original draft, writing–review and editing. **Simhachalam Gurugubelli**: data curation, investigation, methodology, resources, software, roles/writing–original draft, writing–review and editing. **Shahajan Baig**: formal analysis, investigation, validation, visualization, roles/writing–review and editing. **Sunayana Rahul Vikhe**: formal analysis, investigation, validation, visualization, roles/writing–review and editing. **Sachin A. Dhawale**: formal analysis, investigation, validation, visualization, roles/writing–review and editing. **Mohammad Rakib Mortuza**: formal analysis, investigation, validation, visualization, roles/writing–review and editing. **Sherouk Hussein Sweilam**: formal analysis, investigation, validation, visualization, roles/writing–review and editing. **Falak A. Siddiqui**: conceptualization, formal analysis, funding acquisition, investigation, methodology, project administration, supervision, validation, visualization, writing–review and editing. **Sharuk L. Khan**: conceptualization, formal analysis, funding acquisition, investigation, methodology, project administration, supervision, validation, visualization, writing–review and editing. **Marco Tutone**: formal analysis, investigation, validation, visualization, roles/writing–review and editing. **Irfan Ahmad**: formal analysis, investigation, validation, visualization, roles/writing–review and editing. **Md. Zamshed Alam Begh**: formal analysis, investigation, validation, visualization, roles/writing–review and editing.

Acknowledgments

The authors are thankful to their own institutions and to the Deanship of Research and Graduate Studies, King Khalid University, Abha, Saudi Arabia, for financially supporting this work through the Large Research Group Project under Grant No. R.G.P.2/514/45.

Ethics Statement

The authors have nothing to report.

Conflicts of Interest

The authors declare no conflicts of interest.

Data Availability Statement

The data that support the findings of this study are available in the Supporting Information Section of this article.

References

1. B. Gallwitz, "Clinical Use of DPP-4 Inhibitors," *Frontiers Endocrinology (Lausanne)* 10 (2019): 389, https://doi.org/10.3389/fendo.2019.00389.

2. A. B. Olokoba, O. A. Obateru, and L. B. Olokoba, "Type 2 Diabetes Mellitus: A Review of Current Trends," *Oman Medical Journal* 27 (2012): 269–273.

3. T. Y. Tsai, T. Hsu, C. T. Chen, et al., "Rational Design and Synthesis of Potent and Long-Lasting Glutamic Acid-Based Dipeptidyl Peptidase IV Inhibitors," *Bioorganic & Medicinal Chemistry Letters* 19 (2009): 1908–1912.

4. S. Narsimha, K. S. Battula, M. Ravinder, Y. N. Reddy, and V. R. Nagavelli, "Design, Synthesis and Biological Evaluation of Novel 1,2,3-Triazole-Based Xanthine Derivatives as DPP-4 Inhibitors," *Journal of Chemical Sciences* 132 (2020): 59, https://doi.org/10.1007/s12039-020-1760-0.

5. S. S. Abd El-Karim, M. M. Anwar, Y. M. Syam, M. A. Nael, H. F. Ali, and M. A. Motaleb, "Rational Design and Synthesis of New Tetralin-Sulfonamide Derivatives as Potent Anti-Diabetics and DPP-4 Inhibitors: 2D & 3D QSAR, In Vivo Radiolabeling and Bio Distribution Studies," *Bioorganic Chemistry* 81 (2018): 481–493.

6. B. Han, J. L. Liu, Y. Huan, et al., "Design, Synthesis and Primary Activity of Thiomorpholine Derivatives as DPP-IV Inhibitors," *Chinese Chemical Letters* 23 (2012): 297–300.

7. A. L. E. Pereira, G. B. dos Santos, M. S. F. Franco, L. B. Federico, C. da Silva, and C. B. R. Santos, "Molecular Modeling and Statistical Analysis in the Design of Derivatives of Human Dipeptidyl Peptidase IV," *Journal of Biomolecular Structure & Dynamics* 36 (2018): 318–334.

8. B. D. Patel, S. V. Bhadada, and M. D. Ghate, "Design, Synthesis and Anti-Diabetic Activity of Triazolotriazine Derivatives as Dipeptidyl Peptidase-4 (DPP-4) Inhibitors," *Bioorganic Chemistry* 72 (2017): 345–358.

9. R. Tundis, M. R. Loizzo, and F. Menichini, "Natural Products as Alpha-Amylase and Alpha-Glucosidase Inhibitors and Their Hypoglycaemic Potential in the Treatment of Diabetes: An Update," *Mini-Reviews in Medical Chemistry* 10 (2010): 315–331.

10. R. Gupta, S. Walunj, R. Tokala, K. Parsa, S. Singh, and M. Pal, "Emerging Drug Candidates of Dipeptidyl Peptidase IV (DPP IV) Inhibitor Class

for the Treatment of Type 2 Diabetes," *Current Drug Targets* 10 (2009): 71–87.

11. I. M. E. Lacroix and E. C. Y. Li-Chan, "Food-Derived Dipeptidyl-Peptidase IV Inhibitors as a Potential Approach for Glycemic Regulation—Current Knowledge and Future Research Considerations," *Trends in Food Science & Technology* 54 (2016): 1–16.

12. A. Smelcerovic, F. Miljkovic, A. Kolarevic, et al., "An Overview of Recent Dipeptidyl Peptidase-IV Inhibitors: Linking Their Structure and Physico-Chemical Properties With SAR, Pharmacokinetics and Toxicity," *Current Topics in Medicinal Chemistry* 15 (2015): 2342–2372.

13. T. Salvatore, O. Carbonara, D. Cozzolino, R. Torella, and F. Carlo Sasso, "Adapting the GLP-1-Signaling System to the Treatment of Type 2 Diabetes," *Current Diabetes Reviews* 3 (2007): 15–23.

14. R. N. Kushwaha, W. Haq, and S. B. Katti, "Sixteen-Years of Clinically Relevant Dipeptidyl Peptidase-IV (DPP-IV) Inhibitors for Treatment of Type-2 Diabetes: A Perspective," *Current Medicinal Chemistry* 21 (2014): 4013–4045.

15. Y. Liu, Y. Hu, and T. Liu, "Recent Advances in Non-Peptidomimetic Dipeptidyl Peptidase 4 Inhibitors: Medicinal Chemistry and Preclinical Aspects," *Current Medicinal Chemistry* 19 (2012): 3982–3999.

16. F. Salvo, N. Moore, M. Arnaudl, et al., "Addition of Dipeptidyl Peptidase-4 Inhibitors to Sulphonylureas and Risk of Hypoglycaemia: Systematic Review and Meta-Analysis," *BMJ* 353 (2016): i2231, https://doi.org/10.1136/bmj.i2231.

17. A. J. Scheen, "Safety of Dipeptidyl Peptidase-4 Inhibitors for Treating Type 2 Diabetes," *Expert Opinion on Drug Safety* 14 (2015): 505–524.

18. S. H. Tella and M. S. Rendell, "DPP-4 Inhibitors: Focus on Safety," *Expert Opinion on Drug Safety* 14 (2015): 127–140.

19. M. Coghlan and B. Leighton, "Glucokinase Activators in Diabetes Management," *Expert Opinion on Investigational Drugs* 17 (2008): 145–167.

20. M. Pal, "Recent Advances in Glucokinase Activators for the Treatment of Type 2 Diabetes," *Drug Discovery Today* 14 (2009): 784–792.

21. F. M. Matschinsky, B. Zelent, N. Doliba, et al., "Glucokinase Activators for Diabetes Therapy," *Diabetes Care* 34 (2011): S236–S243, https://doi.org/10.2337/dc11-s236.

22. F. M. Matschinsky and D. Porte, "Glucokinase Activators (GKAs) Promise a New Pharmacotherapy for Diabetics," *F1000 Medicine Reports* 2 (2010): 43, https://doi.org/10.3410/M2-43.

23. K. J. Filipski, K. Futatsugi, J. A. Pfefferkorn, and B. D. Stevens, "Glucokinase Activators," *Pharmaceutical Patent Analyst* 1 (2012): 301–311.

24. V. Sekar, S. Chakraborty, S. Mani, V. K. Sali, and H. R. Vasanthi, "Mangiferin From *Mangifera indica* Fruits Reduces Post-Prandial Glucose Level by Inhibiting α-Glucosidase and α-Amylase Activity," *South African Journal of Botany* 120 (2019): 129–134.

25. V. Walia, S. K. Chaudhary, and N. Kumar Sethiya, "Therapeutic Potential of Mangiferin in the Treatment of Various Neuropsychiatric and Neurodegenerative Disorders," *Neurochemistry International* 143 (2021): 104939, https://doi.org/10.1016/j.neuint.2020.104939.

26. N. T. T. Loan, D. T. Long, P. N. D. Yen, T. T. M. Hanh, T. N. Pham, and D. T. N. Pham, "Purification Process of Mangiferin From *Mangifera indica* l. Leaves and Evaluation of Its Bioactivities," *Processes* 9 (2021): 852, https://doi.org/10.3390/pr9050852.

27. M. Sguizzato, F. Ferrara, S. S. Hallan, et al., "Ethosomes and Transethosomes for Mangiferin Transdermal Delivery," *Antioxidants* 10 (2021): 768, https://doi.org/10.3390/antiox10050768.

28. P. T. Lum, M. Sekar, S. H. Gan, V. Pandy, and S. R. Bonam, "Protective Effect of Mangiferin on Memory Impairment: A Systematic Review," *Saudi Journal of Biological Sciences* 28 (2021): 917–927.

29. S. N. Morozkina, T. H. Nhung Vu, Y. E. Generalova, P. P. Snetkov, and M. V. Uspenskaya, "Mangiferin as New Potential Anti-Cancer Agent and Mangiferin-Integrated Polymer Systems—A Novel Research Direction," *Biomolecules* 11 (2021): 1–27.

30. J. Wei, H. Zhang, and Q. Zhao, "In Vitro Inhibitory Effects of Friedelin on Human Liver Cytochrome P450 Enzymes," *Pharmaceutical Biology* 56 (2018): 363–367.

31. T. B. Alves, T. M. Souza-Moreira, S. R. Valentini, C. F. Zanelli, and M. Furlan, "Friedelin in *Maytenus ilicifolia* Is Produced by Friedelin Synthase Isoforms," *Molecules (Basel, Switzerland)* 23 (2018): 700, https://doi.org/10.3390/molecules23030700.

32. C. Sunil, S. S. Irudayaraj, V. Duraipandiyan, S. T. Alrashood, S. A. Alharbi, and S. Ignacimuthu, "Friedelin Exhibits Antidiabetic Effect in Diabetic Rats via Modulation of Glucose Metabolism in Liver and Muscle," *Journal of Ethnopharmacology* 268 (2021): 11365, https://doi.org/10.1016/j.jep.2020.113659.

33. A. B. Furbish, P. Burger, Y. K. Peterson, and P. M. Woster, "434 In Silico ADMET Optimization and Preliminary Biologic Activity of Novel Spermine Oxidase Inhibitors as Neuroprotective Agents," *Journal of Clinical Translation Science* 6 (2022): 85.

34. P. Kaur and G. Khatik, "An Overview of Computer-Aided Drug Design Tools and Recent Applications in Designing of Anti-Diabetic Agents," *Current Drug Targets* 22 (2020): 1158–1182.

35. G. Xiong, Z. Wu, J. Yi, et al., "ADMETlab 2.0: An Integrated Online Platform for Accurate and Comprehensive Predictions of ADMET Properties," Nucleic Acids Research. 2021; 49: W5–W14.

36. A. K. Rappé, C. J. Casewit, K. S. Colwell, W. A. Goddard, and W. M. Skiff, "UFF, a Full Periodic Table Force Field for Molecular Mechanics and Molecular Dynamics Simulations," *Journal of the American Chemical Society* 114 (1992): 10024–10035.

37. A. H. Shntaif, S. Khan, G. Tapadiya, et al., "Rational Drug Design, Synthesis, and Biological Evaluation of Novel N-(2-Arylaminophenyl)-2,3-Diphenylquinoxaline-6-Sulfonamides as Potential Antimalarial, Antifungal, and Antibacterial Agents," *Digital Chinese Medicine* 4 (2021): 290–304.

38. F. A. Siddiqui, S. L. Khan, R. P. Marathe, and N. N. V. Design, "Design, Synthesis, and In Silico Studies of Novel *N*-(2-Aminophenyl)-2,3- Diphenylquinoxaline-6-Sulfonamide Derivatives Targeting Receptor-Binding Domain (RBD) of SARS-CoV-2 Spike Glycoprotein and Their Evaluation as Antimicrobial and Antimalarial Agents," *Letters in Drug Design & Discovery* 18 (2021): 915–931.

39. A. Unnisa, S. L. Khan, F. A. H. Sheikh, et al., "In-Silico Inhibitory Potential of Triphala Constituents Against Cytochrome P450 2E1 for the Prevention of Thioacetamide-Induced Hepatotoxicity," *Journal of Pharmaceutical Research International* 33 (2021): 367–375.

40. S. L. Khan, F. A. Siddiqui, M. S. Shaikh, N. V. Nema, and A. A. Shaikh, "Discovery of Potential Inhibitors of the Receptor-Binding Domain (RBD) of Pandemic Disease-Causing SARS-CoV-2 Spike Glycoprotein From Triphala Through Molecular Docking," *Current Chinese Chemistry* 2, no. 1 (2021): e220321192390, https://doi.org/10.2174/2666001601666210322121802.

41. S. Khan, M. Kale, Siddiqui, and N. Nema, "Novel Pyrimidine-Benzimidazole Hybrids With Antibacterial and Antifungal Properties and Potential Inhibition of SARS-CoV-2 Main Protease and Spike Glycoprotein," *Digital Chinese Medicine* 4 (2021): 102–119.

42. A. Khan, A. Unnisa, M. Sohel, et al., "Investigation of Phytoconstituents of *Enicostemma littorale* as Potential Glucokinase Activators Through Molecular Docking for the Treatment of Type 2 Diabetes Mellitus," *In Silico Pharmacology* 10, no. 1 (2021): 1, https://doi.org/10.1007/s40203-021-00116-8.

43. S. L. Khan, G. M. Sonwane, F. A. Siddiqui, S. P. Jain, M. A. Kale, and V. S. Borkar, "Discovery of Naturally Occurring Flavonoids as Human Cytochrome P450 (CYP3A4) Inhibitors With the Aid of Computational Chemistry," *Indo Global Journal of Pharmaceutical Sciences* 10 (2020): 58–69.

44. R. N. Chaudhari, S. L. Khan, R. S. Chaudhary, S. P. Jain, and F. A. Siddiqui, "B-Sitosterol: Isolation From *Muntingia calabura* Linn Bark Extract, Structural Elucidation and Molecular Docking Studies as Potential Inhibitor of SARS-CoV-2 Mpro (COVID-19)," *Asian Journal of Pharmaceutical and Clinical Research* 13 (2020): 204–209.

45. S. L. Khan and F. A. Siddiui, "Beta-Sitosterol: As Immunostimulant, Antioxidant and Inhibitor of SARS-CoV-2 Spike Glycoprotein," *Archives of Pharmacology and Therapeutics* 2 (2020): 12–16, https://doi.org/10.33696/pharmacol.2.014.

46. K. Park, B. M. Lee, K. H. Hyun, T. Han, D. H. Lee, and H. H. Choi, "Design and Synthesis of Acetylenyl Benzamide Derivatives as Novel Glucokinase Activators for the Treatment of T2DM," *ACS Medicinal Chemistry Letters* 6 (2015): 296–301.

47. A. A. Kazi and V. A. Chatpalliwar, "Design, Synthesis, Molecular Docking and In Vitro Biological Evaluation of Benzamide Derivatives as Novel Glucokinase Activators," *Current Enzyme Inhibition* 18 (2022): 61–75.

48. Q. Min, X. Cai, W. Sun, et al., "Identification of Mangiferin as a Potential Glucokinase Activator by Structure-Based Virtual Ligand Screening," *Scientific Reports* 7 (2017): 44681, https://doi.org/10.1038/srep44681.

49. P. K. Vawhal, S. B. Jadhav, S. Kaushik, et al., "Coumarin-Based Sulfonamide Derivatives as Potential DPP-IV Inhibitors: Pre-ADME Analysis, Toxicity Profile, Computational Analysis, and In Vitro Enzyme Assay," *Molecules (Basel, Switzerland)* 28 (2023): 1004, https://doi.org/10.3390/molecules28031004.

50. P. K. Vawhal and S. B. Jadhav, "Design, Synthesis, and Biological Evaluation of 3-Chloro-2-Oxo-*N*-(Arylcarbamoyl)-2*H*-1-Benzopyran-6-Sulfonamide Derivatives as Potential DPP-IV Inhibitors," *International Journal of Health Sciences* 6 (2022): 373–392.

51. S. Poovitha and M. Parani, "In Vitro and In Vivo α-Amylase and α-Glucosidase Inhibiting Activities of the Protein Extracts From Two Varieties of Bitter Gourd (*Momordica charantia* L.)," *BMC Complementary and Alternative Medicine [Electronic Resource]* 16 (2016): 185, https://doi.org/10.1186/s12906-016-1085-1.

52. Y. I. Kwon, E. Apostolidis, and K. Shetty, "Inhibitory Potential of Wine and Tea Against α-Amylase and α-Glucosidase for Management of Hyperglycemia Linked to Type 2 Diabetes," *Journal of Food Biochemistry* 32 (2008): 15–31.

53. D. E. Shaw, Schrödinger: Desmond Molecular Dynamics System (New York, NY: Schrödinger Release, 2021), 4.

54. S. Dhawale, M. Pandit, K. Thete, et al., "In Silico Approach Towards Polyphenols as Targeting Glucosamine-6-Phosphate Synthase for Candida Albicans," *Journal of Biomolecular Structure & Dynamics* 41 (2023): 12038–12054, https://doi.org/10.1080/07391102.2022.2164797.

55. M. J. Waring, "Lipophilicity in Drug Discovery," *Expert Opinion on Drug Discovery* 5 (2010): 235–248.

56. S. Lobo, "Is There Enough Focus on Lipophilicity in Drug Discovery?," *Expert Opinion on Drug Discovery* 15 (2020): 261–263.

57. G. R. Bickerton, G. V. Paolini, J. Besnard, S. Muresan, and A. L. Hopkins, "Quantifying the Chemical Beauty of Drugs," *Nature Chemistry* 4 (2012): 90–98.

58. T. Kosugi and M. Ohue, "Quantitative Estimate Index for Early-Stage Screening of Compounds Targeting Protein-Protein Interactions," *International Journal of Molecular Sciences* 22 (2021): 10925, https://doi.org/10.3390/ijms222010925.

59. P. Ertl, S. Roggo, and A. Schuffenhauer, "Natural Product-Likeness Score and Its Applications in the Drug Discovery Process," *Chemistry Central Journal* 2 (2008): S1–S2, https://doi.org/10.1186/1752-153x-2-s1-s2.

60. J. Menke, J. Massa, and O. Koch, "Natural Product Scores and Fingerprints Extracted From Artificial Neural Networks," *Computational and Structural Biotechnology Journal* 19 (2021): 4593–4602.

61. O. Ursu, A. Rayan, A. Goldblum, and T. I. Oprea, "Understanding Drug-Likeness," *Wiley Interdisciplinary Reviews: Computational Molecular Science* 1 (2011): 760–781.

62. W. P. Walters, "Going Further Than Lipinski's Rule in Drug Design," *Expert Opinion on Drug Discovery* 7 (2012): 99–107.

63. T. W. Johnson, K. R. Dress, and M. Edwards, "Using the Golden Triangle to Optimize Clearance and Oral Absorption," *Bioorganic & Medicinal Chemistry Letters* 19 (2009): 5560–5564.

64. J. B. Lee, A. Zgair, D. A. Taha, et al., "Quantitative Analysis of Lab-to-Lab Variability in Caco-2 Permeability Assays," *European Journal of Pharmaceutics and Biopharmaceutics* 114 (2017): 38–42.

65. B. Feng, M. West, N. C. Patel, et al., "Validation of Human MDR1-MDCK and BCRP-MDCK Cell Lines to Improve the Prediction of Brain Penetration," *Journal of Pharmaceutical Sciences* 108 (2019): 2476–2483.

66. Y. Persidsky, S. H. Ramirez, J. Haorah, and G. D. Kanmogne, "Blood–Brain Barrier: Structural Components and Function Under Physiologic and Pathologic Conditions," *Journal of Neuroimmune Pharmacology* 1 (2006): 223–236.

67. C. C. Ogu and J. L. Maxa, "Drug Interactions Due to Cytochrome P450," *Baylor University Medical Center Proceedings* 13 (2000): 421–423.

68. X. Pan, "Mutagenicity Evaluation of Nanoparticles by the Ames Assay," *Methods in Molecular Biology* 2326 (2021): 275–285.

69. R. Garg and C. J. Smith, "Predicting the Bioconcentration Factor of Highly Hydrophobic Organic Chemicals," *Food and Chemical Toxicology* 69 (2014): 252–259.

70. J. A. Arnot and F. Gobas, "A Review of Bioconcentration Factor (BCF) and Bioaccumulation Factor (BAF) Assessments for Organic Chemicals in Aquatic Organisms," *Environmental Reviews* 14 (2006): 257–297.

71. T. M. Martin and D. M. Young, "Prediction of the Acute Toxicity (96-h LC50) of Organic Compounds to the Fathead Minnow (*Pimephales promelas*) Using a Group Contribution Method," *Chemical Research in Toxicology* 14 (2001): 1378–1385.

72. A. Tkaczyk, A. Bownik, J. Dudka, K. Kowal, and B. Ślaska, "*Daphnia magna* Model in the Toxicity Assessment of Pharmaceuticals: A Review," *Science of the Total Environment* 763 (2021): 143038, https://doi.org/10.1016/j.scitotenv.2020.143038.

73. P. S. Charifson, J. J. Corkery, M. A. Murcko, and W. P. Walters, "Consensus Scoring: A Method for Obtaining Improved Hit Rates From Docking Databases of Three-Dimensional Structures Into Proteins," *Journal of Medicinal Chemistry* 42 (1999): 5100–5109.

74. P. Kaur, R. C. Gupta, A. Dey, T. Malik, and D. K. Pandey, "Optimization of Harvest and Extraction Factors by Full Factorial Design for the Improved Yield of C-Glucosyl Xanthone Mangiferin From *Swertia chirata*," *Scientific Reports* 11 (2021): 16346, https://doi.org/10.1038/s41598-021-95663-7.

75. F. F. Razura-Carmona, A. Pérez-Larios, N. González-Silva, et al., "Mangiferin-Loaded Polymeric Nanoparticles: Optical Characterization, Effect of Antitopoisomerase I, and Cytotoxicity," *Cancers (Basel)* 11 (2019): 1965, https://doi.org/10.3390/cancers11121965.

76. T. O. Johnson and P. S. Humphries, "Glucokinase Activators for the Treatment of Type 2 Diabetes," *Annual Reports in Medicinal Chemistry* 41 (2006): 141–154.

77. C. F. Deacon, "Dipeptidyl Peptidase 4 Inhibitors in the Treatment of Type 2 Diabetes Mellitus," *Nature Reviews Endocrinology* 16 (2020): 642–653.

78. R. K. Suman, I. R. Mohanty, U. Maheshwari, M. K. Borde, and Y. A. Deshmukh, "Natural Dipeptidyl Peptidase-IV Inhibitor Mangiferin Mitigates Diabetes- and Metabolic Syndrome-Induced Changes in Experimental Rats," *Diabetes, Metabolic Syndrome and Obesity: Targets and Therapy* 9 (2016): 261–272.

79. H. Mechchate, I. Es-Safi, A. Louba, et al., "In Vitro Alpha-Amylase and Alpha-Glucosidase Inhibitory Activity and In Vivo Antidiabetic Activity

of *Withania frutescens* l. Foliar Extract," *Molecules (Basel, Switzerland)* 26 (2021): 293, https://doi.org/10.3390/molecules26020293.

80. G. Oboh, O. B. Ogunsuyi, M. D. Ogunbadejo, and S. A. Adefegha, "Influence of Gallic Acid on α-Amylase and α-Glucosidase Inhibitory Properties of Acarbose," *Journal of Food and Drug Analysis* 24 (2016): 627–634.

Supporting Information

Additional supporting information can be found online in the Supporting Information section.